Acta Pharmaceutica Sinica B 2023;13(9):3906–3918

Chinese Pharmaceutical Association
Institute of Materia Medica, Chinese Academy of Medical Sciences

Acta Pharmaceutica Sinica B

www.elsevier.com/locate/apsb
www.sciencedirect.com

ORIGINAL ARTICLE

Amelioration of ethanol-induced oxidative stress and alcoholic liver disease by *in vivo* RNAi targeting *Cyp2e1*

Yalan Wang[a,†], Qiubing Chen[b,c,†], Shuang Wu[a], Xinyu Sun[a], Runting Yin[a], Zhen Ouyang[a], Hao Yin[b,c,d,e,f,*], Yuan Wei[a,*]

[a]*School of Pharmacy, Jiangsu University, Zhenjiang 212013, China*
[b]*Department of Urology, Frontier Science Centre for Immunology and Metabolism, Medical Research Institute, Zhongnan Hospital of Wuhan University, Wuhan University, Wuhan 430071, China*
[c]*Department of Pulmonary and Critical Care Medicine, Zhongnan Hospital of Wuhan University, Wuhan 430071, China*
[d]*Department of Pathology, Zhongnan Hospital of Wuhan University, Wuhan 430071, China*
[e]*RNA Institute, Wuhan University, Wuhan 430072, China*
[f]*Wuhan Research Centre for Infectious Diseases and Cancer, Chinese Academy of Medical Sciences, Wuhan 430010, China*

Received 26 September 2022; received in revised form 16 November 2022; accepted 10 December 2022

KEY WORDS

Alcoholic liver disease;
RNAi;
Lipid nanoparticle;
Cyp2e1;
Reactive oxygen species;
Oxidative stress;
Lipogenesis;
Lipometabolism

Abstract Alcoholic liver disease (ALD) results from continuous and heavy alcohol consumption. The current treatment strategy for ALD is based on alcohol withdrawal coupled with antioxidant drug intervention, which is a long process with poor efficacy and low patient compliance. Alcohol-induced CYP2E1 upregulation has been demonstrated as a key regulator of ALD, but *CYP2E1* knockdown in humans was impractical, and pharmacological inhibition of CYP2E1 by a clinically relevant approach for treating ALD was not shown. In this study, we developed a RNAi therapeutics delivered by lipid nanoparticle, and treated mice fed on Lieber-DeCarli ethanol liquid diet weekly for up to 12 weeks. This RNAi-based inhibition of *Cyp2e1* expression reduced reactive oxygen species and oxidative stress in mouse livers, and contributed to improved ALD symptoms in mice. The liver fat accumulation, hepatocyte inflammation, and fibrosis were reduced in ALD models. Therefore, this study suggested the feasibility of RNAi targeting to *CYP2E1* as a potential therapeutic tool to the development of ALD.

*Corresponding authors.
E-mail addresses: haoyin@whu.edu.cn (Hao Yin), ywei@ujs.edu.cn (Yuan Wei).
[†]These authors made equal contributions to this work.
Peer review under the responsibility of Chinese Pharmaceutical Association and Institute of Materia Medica, Chinese Academy of Medical Sciences.

https://doi.org/10.1016/j.apsb.2023.01.009

1. Introduction

Alcoholic liver disease (ALD) refers to a series of liver diseases, including alcoholic fatty liver (AFL), alcoholic hepatitis, and alcoholic liver fibrosis, that are caused by long-term alcohol consumption[1,2]. Liver damage occurs progressively throughout the ALD stages. Approximately 90%−95% of long-term alcohol drinkers will experience fat accumulation in the liver and develop AFL. About 10%−35% of the patients with AFL will develop alcoholic hepatitis[3]. Moreover, 20%−40% of patients with AFL may develop alcoholic liver fibrosis as their condition worsens. Furthermore, upon continuous alcohol consumption, 10%−15% of patients with alcoholic liver fibrosis may progress to alcoholic cirrhosis[4] and 3%−10% of the cases may further progress to liver cancer[5]. Liver injury is progressively aggravated with continuous alcohol intake[6]. However, there are few specific effects available for the treatment of ALD, Glucocorticoids are often used alone or in combination with Pentoxifylline for the treatment of ALD, but Glucocorticoids have significant side effects[7] and are not suitable for long-term treatment. Metadoxine is commonly used to treat acute alcoholism[8], but does not directly improve liver function. Natural antioxidant compounds such as silybin can repair the liver by attenuating lipid peroxidation reactions[9], and although toxicity and side effects are low, their low bioavailability and rapid metabolic rate make them disappear from the body quickly[10]. The clinical treatment strategy for ALD is alcohol withdrawal coupled with drug intervention[11], which is a long process with poor efficacy and low patient compliance.

The protein CYP2E1, a member of the cytochrome P450 family was confirmed as a vital enzyme responding to long-term ethanol consumption and the development of ALD[12−15]. The levels of CYP2E1 protein and the associated mRNA were significantly upregulated in the livers of patients drinking alcohol and in rodents after long-term ethanol consumption[16,17]. The metabolism of ethanol by CYP2E1 generates large amounts of reactive oxygen species (ROS)[18], leading to oxidative stress[19]. Chronic administration of alcohol to rats can significantly induce the expression of CYP2E1 in their livers and aggravate liver fibrosis[20]. There have been studies that inhibited the development of ALD by constructing *Cyp2e1* knockout mice and exacerbated the effects of alcohol-induced liver injury in humanized *CYP2E1* knock-in mice[21−23]. And the inhibition of CYP2E1 by the specific inhibitor, clotrimazole[24], improved ALD[25]. These studies collectively demonstrate the relevance of CYP2E1 as a key effector in ALD development and the therapeutic effect on ALD may be achieved by inhibiting CYP2E1. However, *CYP2E1* knockout can hardly be achieved clinically. And chemical inhibitor clotrimazole has an inhibitory effect not only on CYP2E1, but also on other cytochrome P450s such as CYP2B6 and CYP2A6[26]. Clotrimazole-related adverse effects have been clinically found to be numerous[27,28] and potentially addictive[29].

RNA-interference (RNAi) therapeutics is to silence specific target gene(s) to block their protein expression *in vivo* to treat diseases[30,31]. RNAi technology has been demonstrated for the treatment of diabetes[32], myocardial ischemia[33], acute lung injury[34], cancer[35], and kidney disease[36] in animal models. Recently several drugs based on RNAi have been approved by FDA, making RNAi therapeutics viable, particularly for targeting liver-related diseases. Lipid nanoparticles (LNP) encapsulated chemically modified siRNA (LNP-siRNA) was used for the FDA approved RNAi therapeutics.

In this study, we developed a novel LNP-siRNA method to specifically knockdown *Cyp2e1* in mouse livers. Therapeutical effects on ALD were observed in those alcohol-treated mouse models, and this RNAi-based method showed good potentials as a new therapeutic tool.

2. Materials and methods

2.1. Materials

Lieber-DeCarli diet was purchased from Dyets Biotechnology (Wuxi, China). Dlin-MC3-DMA, disteroylphosphatidyl choline, and cholesterol were purchased from AVT (Shanghai, China). C14-PEG2000 was purchased from Sigma−Aldrich (Shanghai, China). Silybin glucosamine (≥98% purity) was gifted by Jiangsu Zhongxing Pharmaceutical (Jiangsu, China). Analysis kits for alanine aminotransferase (ALT), aspartate transaminase (AST), reactive oxygen species (ROS), malondialdehyde (MDA), superoxide dismutase (SOD), glutathione (GSH), glutathione peroxidase (GSH-Px), triglyceride (TG), total cholesterol (TC), and hydroxyproline (HYP) were obtained from Nanjing Jiancheng Bioengineering Institute (Nanjing, China). The expression of interleukin-6 (IL-6) and Tumor necrosis factor alpha (TNF-α) in mouse serum were detected by ELISA kits were obtained from BYabscience (Nanjing, China). RIPA buffer, BCA protein concentration analysis kits, and Horseradish peroxidase (HRP)-labeled goat anti-rabbit IgG (H&L), BeyoRT™ cDNA First Strand Synthesis Kit, and BeyoFast™ SYBR Green qPCR Mix were purchased from The Beyotime Institute of Biotechnology (Shanghai, China). An anti-Cyp2e1 antibody (BML-CR3271) was purchased from Enzo Biochem (New York, NY, USA). Acetyl-CoA carboxylase (ACC, PAB284Mu01), carnitine palmitoyltransferase 1 (CPT1, PAF368Mu01), fatty acid synthase (FAS, PAC470Mu01), sterol regulatory element binding protein-1c (SREBP1c, PAC868Mu01), and peroxisome proliferator-activated receptor-γ coactivator-1α (PGC-1α, PAH337Mu01) antibodies were obtained from CLOUD-CLONE CORP. (Wuhan, China). Calnexin antibody (10427-2-AP) was obtained from Proteintech Group (Wuhan, China), GAPDH antibody (ab9485) was obtained from Abcam (Cambridge, MA, USA), and β-actin antibody (orb-10033) was obtained from Biorbyt (Wuhan, China). Polyvinylidene fluoride (PVDF) membranes were purchased from Millipore (Billerica, MA, USA). Lipofectamine™ RNAiMAX and Trizol reagent was sourced from Thermo Fisher Scientific (Waltham, MA, USA). All reagents and solvents were of analytical grade.

2.2. siRNA design, synthesis, and screening

Four siRNAs targeting mouse *Cyp2e1* were designed and used as previously described[37]. Single-stranded RNAs, which had 2′-*O*-methyl modifications and dTsdT 3′ overhangs ("s" indicates phosphorothioate linkage) to improve RNA stability *in vivo* and inhibit immune stimulation, were produced at GenScript (Nanjing, China). The equimolar amounts of complementary strands were mixed in an annealing buffer (50 mmol/L Tri-HCl buffer, 100 mmol/L NaCl, pH 8.0). Then, they were heated at 95 °C for 5 min and slowly cooled to 25 °C at a rate of 0.1 °C/s using PCR.

Since the low expression of CYP2E1 protein in conventional hepatocyte cell lines did not achieve a good screening effect, screening experiments were performed by constructing a *Cyp2e1* overexpressing stable cell line (Cyp2e1 OE cells). Hepa 1−6 cells were cultured in DMEM supplemented with 10% FBS and cultured in a humidified incubator at 37 °C with 5% CO_2. Stable cell lines overexpressing the CYP2E1 protein were obtained through transfection with a lentiviral vector for 48 h, as previously described[38]. After puromycin screening, Cyp2e1 OE cells were finally constructed and identified using qRT-PCR and western blotting.

Cyp2e1 OE cells were seeded at a seeding density of 1.0×10^5 cells per well in 24-well plates. Meanwhile, *Cyp2e1* siRNAs were transfected using lipofectamine™ RNAiMAX transfection reagent for 24 h. The knockdown efficacy of *Cyp2e1* was measured by qRT-PCR, and IC_{50} values were calculated.

2.3. Preparation and characterization of LNPs

The LNPs were prepared using a microfluidic device according to the previously reported procedure[39]. Briefly, Dlin-MC3, DSPC, cholesterol, and C14-PEG2000 were dissolved in ethanol at a of 50/10/38.5/1.5 (*m*/*m*/*m*/*m*), respectively, and siRNAs were dissolved in 10 mmol/L citrate buffer. Then, the lipid and siRNAs were mixed in a ratio of 1/3 (*n*/*n*) through the microfluidic device at a rate of 12 mL/min. Finally, the mixture was dialyzed against PBS (pH 7.4) for 2 h to remove alcohol using a 100,000 MWCO membrane at 25 °C. Particle size distribution and polydispersity index (PDI) were measured using a Malvern Nano ZS90 (Malvern Instruments, Ltd., Worcestershire, UK). The siRNA encapsulation efficiency was determined by Quant-iT™ RiboGreen™ RNA Assay (Thermo Fisher Scientific) in the presence and absence of Triton X-100 (1%, *v*/*v*) as reported in the published methods[37].

2.4. Animal experiments

Female C57BL/6N mice aged 6−8 weeks weighing 20 ± 2 g were collected from Vital River Laboratories (Beijing, China). Mice were housed at the Jiangsu University Experimental Animal Center (Zhenjiang, China) and were allowed to adapt to laboratory environments (25 ± 2 °C, 40% relative humidity, 12 h light/dark cycle) for 5 days. The animal facilities at Jiangsu University have passed the certification of the Association for Assessment and Accreditation of Laboratory Animal Care. All animal breeding and experimental procedures were performed in accordance with the Guide for the Care and Use of Laboratory Animals and were approved by the Institutional Animal Care and Use Committees at Jiangsu University.

2.4.1. Knockdown efficiency of si-Cyp2e1 LNPs in vivo

To verify the knockdown effect of si-*Cyp2e1* in mice, the mice were injected with 0.5 mg/kg LNPs-formulated si-*Cyp2e1* (si-*Cyp2e1* LNPs) or si-*Control* (si-Control LNPs) in PBS by tail vein injection[37]. There were five mice in each group. Animals received one injection and the expression of CYP2E1 in mice was detected on Days 1, 3, 5, 7, and 10 after injection. The group injected with PBS was labeled as the negative control.

2.4.2. si-Cyp2e1 LNPs treatment of ALD in mice

NIAAA model[40] is a recently established chronic alcohol-fed mouse model that efficiently mimics the characteristics of different stages of human ALD. In this study, the NIAAA model of ALD induction was established as previously reported[40−42], with modifications to assess the effect of si-*Cyp2e1* LNPs on ALD development. Briefly, 8-week-old C57BL/6N female mice were divided into alcohol-fed, pair-fed, and nine administration groups as indicated in Fig. 1, where each group is composed of six mice. First, each group of mice was fed with an equal caloric transition for one week, ensuring that the energy intake of each group was as equal as possible. The mice in the alcohol-fed group and administration groups were fed with increasing alcohol concentrations of Lieber-DeCarli liquid diet[43] to allow the mice to gradually adapt to alcohol irritation, with the alcohol concentration eventually reaching 4%. Then, mice received an *ad libitum* diet of Lieber-DeCarli liquid with 4% ethanol for 12 weeks plus multiple binges (twice a week) of ethanol (5 g/kg, b.w.). Pair-fed animals received a calorie-matched liquid diet.

Three administration groups received treatment lasting for 12 weeks ("early treatment" cohort; ET): one group received once-weekly tail vein injections of 0.5 mg/kg of si-*Cyp2e1* LNPs; one group received once-weekly tail vein injections of 0.5 mg/kg of si-*Control* LNPs; and the other group received daily gavage of 100 mg/kg of silybin glucosamine. The following three administration groups received treatment lasting for 8 weeks (beginning at week 5 to 12 of alcohol feeding; "mid-treatment" cohort; MT): refers to the three administration groups of the "early treatment" cohort. The last three administration groups received treatment lasting for 4 weeks (beginning at week 9 to 12 of alcohol feeding; "late-treatment" cohort; LT): refer to the three administration groups of the "early treatment" cohort. Silybin glucosamine was used as the positive control.

2.5. RNA analysis

Total RNA was extracted from the liver tissues of the mice using TRIzol reagent according to the manufacturer's instructions. Reverse transcription was performed at 42 °C for 60 min, followed by 70 °C for 5 min, according to the BeyoRT™ cDNA First Strand Synthesis Kit manufacturer's instructions. The reaction product was stored at −20 °C. The qRT-PCR experiments were performed using a BeyoFast™ SYBR Green qPCR Mix and a Light Cycle 96 Real-Time PCR system (Roche, Basel, Switzerland). The qRT-PCR program comprised a reverse transcription step at 48 °C for 30 min, and a Taq polymerase activation step at 95 °C for 300 s. This was followed by DNA chains elongation reactions: 45 cycles at 95 °C for 15 s, 61 °C for 20 s, and 72 °C for 30 s, followed by a final melting cycle at 95 °C for 15 s, 60 °C for 15 s, and 95 °C for 15 s. Gene expression levels in each sample were determined using the $2^{-\Delta\Delta Ct}$ method[44], normalized to the expression levels of the housekeeping gene, *GAPDH*. The primer sequences are shown in Supporting Information Table S1.

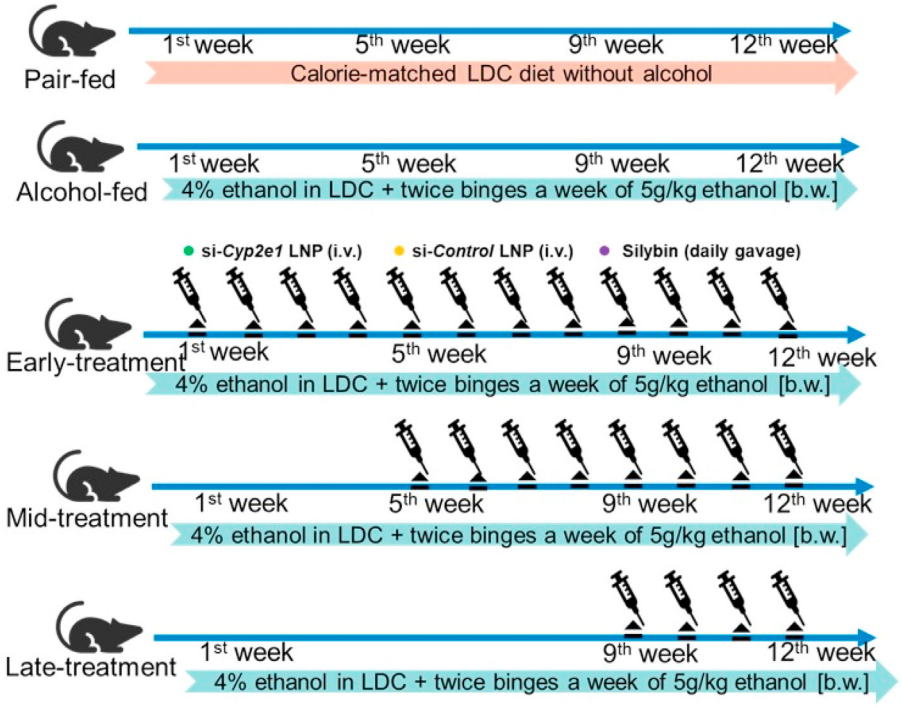

Figure 1 Schematic representation of the experiment, timeline of repeated injections of LNP-formulated siRNA.

2.6. *Protein analysis*

Mouse liver microsomes were prepared using differential centrifugation[45], the total protein of mouse liver and cultured cells were lysed in RIPA buffer according to the manufacturer's instructions. BCA protein concentration analysis kits were used to determine the protein concentrations in the microsome suspensions. The protein expression of CYP2E1 in liver microsomes and cells was detected by western blotting. The protein expression of SREBP1c, FAS, ACC, PGC-1α and CPT1 in mouse liver total protein were also detected by western blotting. Equal amounts of protein from liver microsomes (5 μg)[46] or total protein (30 μg) were separated by sodium dodecyl sulfate-polyacrylamide gel electrophoresis and then transferred onto PVDF membranes. The membranes were probed with antibodies overnight at 4 °C and then incubated with an HRP-coupled secondary antibody. The protein bands were detected using enhanced chemiluminescence reagents. Chemiluminescent signals were visualised and analysed using a ChemiDoc XRS imaging system (Bio-Rad, Hercules, CA, USA). Calnexin was used as a loading control for microsome samples and β-actin was used as a loading control for total cell lysis samples. GAPDH was used as a loading control for mouse liver total protein.

2.7. *Measurement of mouse liver index and biochemical assays*

The mouse liver index was calculated according to the following Eq. (1):

$$\text{Index}_{\text{ml}} = 100 \times W_{\text{lv}}/W_{\text{bw}} \quad (1)$$

where Index_{ml} is mouse liver index, W_{lv} is liver wet weight, W_{bw} is body weight.

Blood samples were collected after eyeball removal, and the serum was prepared by centrifugation (900×*g*, 10 min). The serum levels of ALT and AST were measured using enzymatic assay kits according to the manufacturer's instructions. The serum levels of IL-6 and TNF-α were measured using ELISA kits according to the manufacturer's instructions. Liver homogenates were prepared from liver tissues with ice-cold saline (1/9, *w*/*w*), and liver ROS, GSH, MDA, SOD, GSH-Px, HYP, TG, and TC concentrations were determined using the respective detection kits according to the manufacturer's instructions. The ROS values of each group were normalized to the ratio with the pair-fed group.

2.8. *Liver histomorphology*

Two 5-mm liver tissue sections of each mouse were taken and cut. One was fixed in 4% paraformaldehyde for 24 h and was then embedded in paraffin. The other was snap-frozen in liquid N_2 and stored at −80 °C till further use. Paraffin sections were stained with hematoxylin-eosin (H&E), Sirius red, and fluorescent immunomarkers. Macrophage infiltration was analyzed by fluorescent immunohistochemical staining F4/80 (Bio-Rad; Hercules, California), at least 6 randomly selected 200× fields of view for each section within each group were photographed. The photographs were taken so that the tissue filled the entire field of view as much as possible, ensuring that the background light was consistent in each photograph. Image-Pro Plus 6.0 (Media Cybernetics, MD, USA) software was used to convert the green/red fluorescent monochrome photos into black and white images and then selected the same black color as the uniform standard for judging the positivity of all photos, and each photo was analyzed to obtain the cumulative optical density (IOD) value for each positive photo. Frozen sections were thawed to room temperature for oil red O staining and microscopic observation of liver lipid accumulation. The area of fat accumulation in the liver within the same field of view of frozen sections was measured using Image-Pro (Media Cybernetics, MD, USA) image analysis software to quantify fat hoarding in the liver, and six 200× fields of view were selected for mean value analysis.

2.9. Statistical analysis

All data are expressed as the mean ± standard deviation (SD). The data were evaluated for statistical significance by one-way analysis of variance (ANOVA) using SPSS 13.0 (IBM, Armonk, NY, USA), and $P < 0.05$ was considered to be statistically significant.

3. Results

3.1. Establishment of ALD mouse model

To characterize chronic alcohol intake at different time periods, as shown in the Supporting Information Fig. S1, we assessed liver damage in female C57BL/6N mice subjected to 4 weeks (E4w + nB), 8 weeks (E8w + nB) and 12 weeks (E12w + nB) of alcohol treatment. The results showed that alcohol intake induced a significant increase in liver index, serum AST and ALT, a significant increase in liver TG, TC and MDA levels, and a significant decrease in liver SOD and GSH levels in mice (Supporting Information Table S3). H&E results showed that mice in the alcohol model group all showed a large amount of steatosis and cell necrosis, and oil red O results showed that alcohol intake led to a large accumulation of lipid droplets in hepatocytes (Supporting Information Fig. S2). The results of quantitative analysis of oil red o staining (Supporting Information Table S3) showed that the liver fat content exceeded 12% after 4 weeks of alcohol treatment, 18% after 8 weeks of alcohol treatment, and 25% when the alcohol treatment reached 12 weeks. The results indicated that this modeling method led to liver injury and oxidative stress in mice, resulting in hepatic fat accumulation and successful construction of an ALD model, and different degrees of alcoholic fatty liver with prolonged alcohol treatment time.

3.2. Optimization of active siRNA molecules targeting *Cyp2e1*

Chemically modified siRNAs targeting *Cyp2e1* were designed and screened (Table 1). The control sequence was described by Akinc et al.[47]. siRNAs targeting *Cyp2e1* were selected and synthesized, which had 2′-O-methyl modifications and dTsdT 3′-overhangs ("s" indicates phosphorothioate linkage) to improve the RNA stability *in vivo* and inhibit the immune stimulation. Cyp2e1 OE cells stably expressed CYP2E1 was constructed to examine the efficiency of siRNA (Fig. 2A). Then, the gene silencing efficiency for each siRNA was examined at 10 nmol/L. Three siRNAs targeting *Cyp2e1* can achieve profound knockdown at this dose (Fig. 2B). A dose−response study was performed and the most potent siRNA targeting *Cyp2e1* was selected (si-*Cyp2e1*-3, IC_{50} ~0.0005 nmol/L) (Fig. 2C). Approximately 90% of *Cyp2e1* mRNAs knockdown was reached after si-*Cyp2e1*-3 transfection (Fig. 2D), and CYP2E1 protein levels were almost diminished 48 h after treatment (Fig. 2E).

3.3. Characterization and knockdown effects of si-Cyp2e1 LNPs in vivo

The si-*Cyp2e1*-3 was selected and si-*Cyp2e1* LNPs were prepared and characterized (Fig. 3A). The expression levels of *Cyp2e1* were evaluated in mouse livers at different time points after a single injection. Real-time PCR analysis confirmed that the hepatic expression of *Cyp2e1* mRNA was reduced by 90% on day 1 after LNP-siRNA injection. As RNAi inhibition is reversible levels after 10 days (Fig. 3B, $P < 0.01$). Western blot results showed that CYP2E1 protein levels decreased to 30% one day after injection and remained at 70% on Day 7 after injection (Fig. 3C, $P < 0.01$ and 3D). Based on the silencing effect of si-*Cyp2e1* LNPs in mice, ALD treatment was performed using a weekly dosing regimen.

3.4. Effects of si-Cyp2e1 LNPs on chronic alcohol-induced liver injury

After confirming the significant knockdown of si-*Cyp2e1* LNPs on hepatic Cyp2e1 expression in mice, si-*Cyp2e1* LNPs were injected at different stages of ALD in mice. The liver index, serum, and liver samples' biochemical analyses of each group of mice were examined. The effects of si-*Cyp2e1* LNPs on alcoholic liver injury in mice are shown in Fig. 4.

The results showed that the liver index of mice in the alcohol-fed group was significantly higher compared to the pair-fed group (Fig. 4A, $P < 0.01$), while the liver index of mice was significantly lower after the administration of si-*Cyp2e1* LNPs than in the alcohol-fed group (Fig. 4A, $P < 0.01$). This indicates that chronic alcohol consumption induced an increase in the liver index, and si-*Cyp2e1* LNPs were able to attenuate this injury.

Serum AST, ALT, IL-6 and TNF-α levels in the alcohol-fed group were also significantly higher than those in the pair-fed group (Fig. 4B−E, $P < 0.01$). Moreover, the AST, ALT, IL-6 and TNF-α levels of mice after the administration of si-*Cyp2e1* LNPs were significantly lower than those in the alcohol-fed group (Fig. 4B and C, $P < 0.01$), indicating that si-*Cyp2e1* LNPs were able to suppress the alcohol-induced elevation of AST, ALT, IL-6 and TNF-α levels in mice. The protective effect of si-*Cyp2e1* LNPs on the alcohol-induced liver injury was significant, where the most pronounced protective effect was observed in the early-treatment group. The protective effect was more pronounced with

Table 1 Sequences of siRNAs targeting *Cyp2e1*.

Gene	siRNA name	Sequence
Cyp2e1	si-*Cyp2e1*-1 sense	5′-cuuucuuuGGAAAcAuuuudTsdT-3′[a]
	si-*Cyp2e1*-1 antisense	5′-AAAAUGUUUCcAAAGAAAGdTsdT-3′
	si-*Cyp2e1*-2 sense	5′-ccAcAGAAAAGucAuGAAAdTsdT-3′
	si-*Cyp2e1*-2 antisense	5′-UUUcAUGACUUUUCUGUGGdTsdT-3′
	si-*Cyp2e1*-3 sense	5′-ccAuGuAcAcAAuGGAAAAdTsdT-3′
	si-*Cyp2e1*-3 antisense	5′-UUUUCcAUUGUGuAcAUGGdTsdT-3′
	si-*Cyp2e1*-4 sense	5′-cccAGAAAuuGAAGAGAAAdTsdT-3′
	si-*Cyp2e1*-4 antisense	5′-UUUCUCUUcAAUUUCUGGGdTsdT-3′
Control	si-Control sense	5′-cuuAcGcuGAGuAcuucGAdTsdT-3′
	si-Control antisense	5′-UCGAAGuACUcAGCGuAAGdTsdT-3′

[a]The 2′-OMe modified nucleotides are in lower case, and the phosphorothioate linkages are indicated by "s".

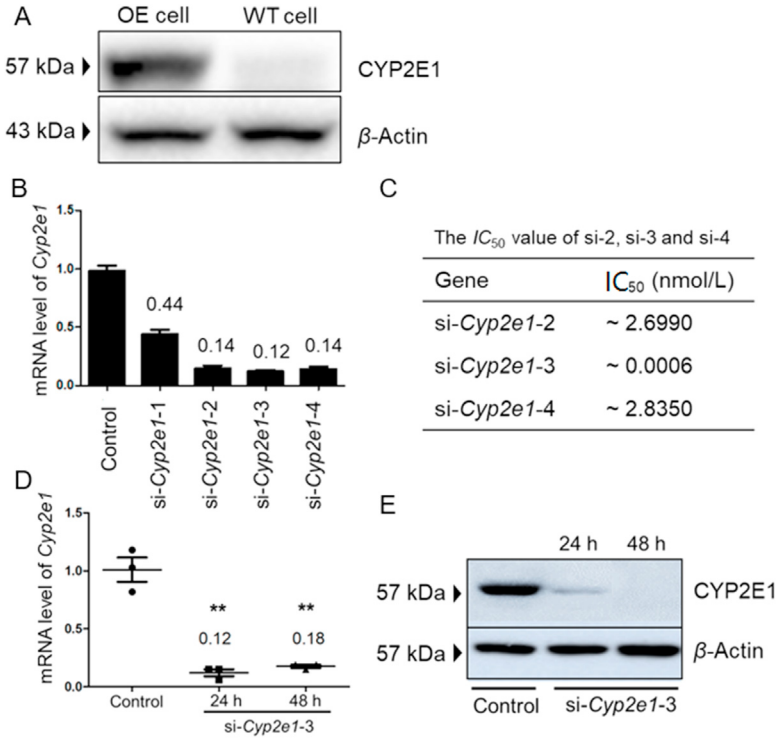

Figure 2 *Cyp2e1* siRNA *in vitro* screening. (A) The protein expression levels of Cyp2e1 in Cyp2e1 OE cells; (B) The silencing levels of 4 siRNAs at a concentration of 10 nmol/L; (C) The IC_{50} of si-2, si-3 and si-4; (D and E) The silencing levels of si-*Cyp2e1*-3 transfected cells 1 and 2 days after transfection. Each value is the group mean ± SD ($n = 5$). One-way ANOVA with Student's *t*-test. Asterisks represent statistical difference between Control and *Cyp2e1* siRNA-treated groups; $^{**}P < 0.01$ *vs.* control.

the earlier administration of the drug and when AST was maintained at the pair-fed level.

Histological evaluation by H&E staining of liver sections showed that the control treatment resulted in no apparent abnormalities (Fig. 4G). From the H&E staining results of the liver tissues of the mice in each group, it could be seen that the hepatocytes of the mice in the pair-fed group were neatly arranged, the structure of the liver lobules was intact, and no balloon-like degeneration was observed. Compared with the pair-fed mice, the alcohol-fed mice had disorganized liver tissues with severe steatosis and inflammatory cell infiltration. Compared with the alcohol-fed group, the liver tissue morphology of si-*Cyp2e1* LNPs-treated mice in each group was improved and steatosis was significantly reduced.

Macrophage infiltration was analyzed by F4/80 fluorescent immunohistochemical staining. As shown in Fig. 4H, alcohol significantly induces inflammatory cell infiltration, and administration of si-*Cyp2e1* LNPs attenuates this inflammation to a greater extent. This result was also verified by the quantitative F4/80 fluorescence analysis (Fig. 4F).

The protective effect of si-*Cyp2e1* LNPs on alcohol-induced liver injury was significant, where the most pronounced protective effect was observed in the early-treatment group and was proportional with the earlier administration of the drug.

3.5. *Effects of si-Cyp2e1 LNPs on oxidative stress and liver lipid levels in ALD*

The levels of liver ROS and MDA in the alcohol-fed group was significantly higher than that in the pair-fed group (Fig. 5A and E, $P < 0.01$). The GSH, GSH-Px, and SOD antioxidant indexes were significantly decreased in the alcohol-fed group (Fig. 5B−D, $P < 0.01$), while si-*Cyp2e1* LNPs could significantly reverse these changes (Fig. 5A−E, $P < 0.01$).

The liver TG and TC levels of each group were measured. As shown in Fig. 5, the liver TG and TC levels in alcohol-fed mice were significantly higher than those in the pair-fed group (Fig. 5G and H, $P < 0.01$), indicating that alcohol induces lipid metabolism disorders in the liver. Treatment with si-*Cyp2e1* LNPs significantly reduced both liver TG and TC levels after administration (Fig. 5G and H, $P < 0.01$), with better results observed in the early-treatment group.

Further histological evaluation by oil red O staining (Fig. 5J), showed that chronic alcohol feeding led to a high accumulation of lipid droplets in the livers of mice, while si-*Cyp2e1* LNPs significantly reduced fat accumulation in the liver. The area of fat accumulation in the same visual field of the frozen section was measured by Image-Pro image analysis software to quantify the retention of fat in the liver. The results showed that the extent of liver fat accumulation in alcohol-fed mice was significantly higher than that in the pair-fed group and the si-*Cyp2e1* LNPs group (Fig. 5I, $P < 0.01$).

The liver HYP levels of each group were measured. The liver HYP levels in alcohol-fed mice were significantly higher than those in the pair-fed group, while si-*Cyp2e1* LNPs could significantly reverse these changes (Fig. 5F, $P < 0.01$). The results of Sirius red staining showed that after 12 weeks of alcohol feeding, the mice developed slight liver fibrosis, and si-*Cyp2e1* LNPS significantly improved liver fibrosis when administered at different stages of ALD (Fig. 5K).

si-*Cyp2e1* LNPs could effectively reduce the alcohol-induced lipid disorders in liver tissues. These indicators were most

A Characterization of si-*Cyp2e1* LNPs

Parameter	Value
Size (nm)	73.77±0.22
PDI	0.04
Encapsulation efficiency (EE)	88.04±0.28

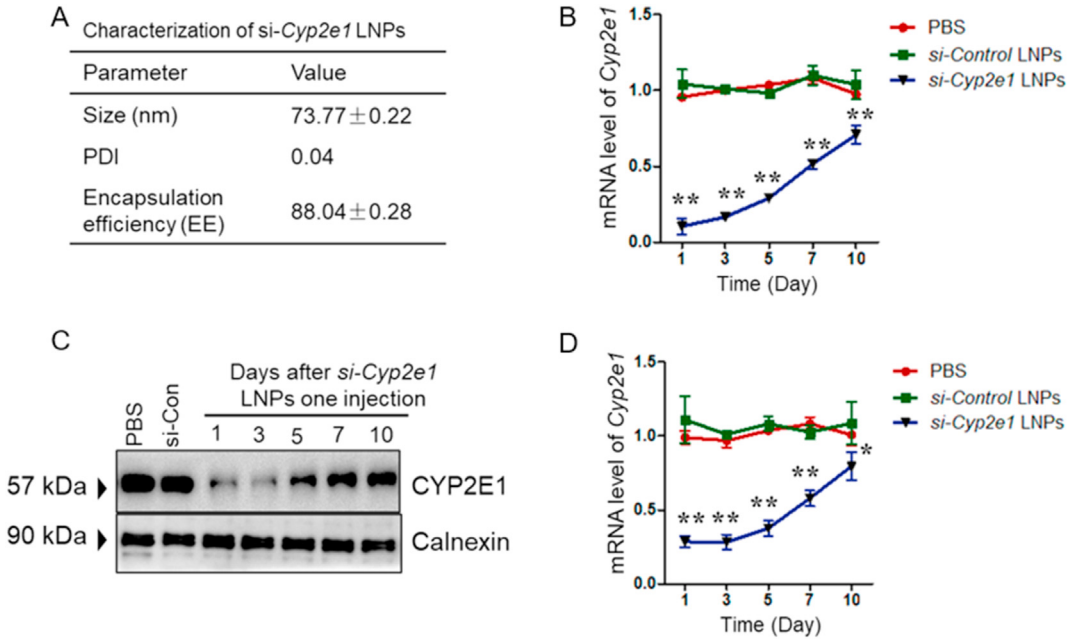

Figure 3 Knockdown effects of si-*Cyp2e1* LNPs *in vivo*. (A) Characterization of si-*Cyp2e1* LNPs. (B) mRNA level of *Cyp2e1* in mice at different time points after a single injection of 0.5 mg/kg si-*Cyp2e1* LNPs ($n = 5$). (C) and (D) Protein level of Cyp2e1 in mice at different time points after a single injection of 0.5 mg/kg si-*Cyp2e1* LNPs ($n = 5$). Each value is the group mean ± SD ($n = 5$). One-way ANOVA with Student's *t*-test. Asterisks represent statistical difference between PBS and *Cyp2e1* siRNA-treated groups; $^*P < 0.05$ and $^{**}P < 0.01$ *vs*. control.

evident in the mice in the early-treatment group, where the liver tissue has a similar structure to that of the blank control group, with significant improvements in fat vacuoles, inflammatory cell infiltration, lipid droplet accumulation, liver fibrosis status, and inflammation.

3.6. Effect of si-Cyp2e1 LNPs on the expression of genes related to oxidative stress and steatosis

Mouse liver microsomes, total RNA and total protein were prepared from the livers of mice in the pair-fed group, alcohol-fed group, si-*Cyp2e1* LNPs (early-treatment) group, and si-Control LNPs (early-treatment) group at the end of animal treatment. After 12 weeks of alcohol feeding, CYP2E1 protein expression was elevated approximately by 2.14-fold in the alcohol-fed group compared to the pair-fed group. Whereas after 12 weeks of continuous administration of si-*Cyp2e1* LNPs by tail vein injection, there was a decrease of >39% in the Cyp2e1 protein expression (Fig. 6A and B, $P < 0.01$).

The expression of depletion-related genes and generation-related genes of ROS are shown in Fig. 6C and D. The results showed that si-*Cyp2e1* LNPs inhibited the increase of alcohol-induced expression of *P47phox*, *P67phox*, and *Gp91phox* ($P < 0.01$), and restored the expression of *Gshpx*, *Gshrd*, and *Sod1* to its normal level ($P < 0.01$). The mRNA expression of inflammatory factors was also examined, and the results showed that alcohol induced the expression of *Il-6*, *Tnf-α*, and *Tgf-β*, while si-*Cyp2e1* LNPs restored this induced expression (Fig. 6E, $P < 0.01$).

The metabolic pathway regulating fat synthesis and fatty acid oxidation *in vivo* can control fatty acid metabolism and fat retention in the liver. Therefore, the expression of genes responsible for regulating lipid metabolism in the liver was further analyzed to verify the possible mechanism of si-*Cyp2e1* LNPs on the regulation of ALD in mice. The results showed that the expression of the fatty acid synthesis-related genes *Srebp1c*, *Acc*, and *Fas* was upregulated by alcohol feeding (Fig. 6F, $P < 0.01$), and the expression of the fatty acid oxidation-related genes *Cpt1* and *Pgc-1α* was significantly decreased (Fig. 6G, $P < 0.01$). Corresponding protein expression levels were consistent with mRNA expression levels (Fig. 6H, $P < 0.01$). In contrast, the administration of si-*Cyp2e1* LNPs significantly increased the expression of the fatty acid oxidation-related genes and decreased the expression of the lipid synthesis-related genes (Fig. 6F–H, $P < 0.01$).

4. Discussion

CYP2E1 is a key enzyme that plays a role in the incidence and development of most liver diseases, in addition to its role in the response to drug toxicity. Furthermore, CYP2E1 has a key role in ALD and plays an important role in the pathological process of non-alcoholic liver disease[48], Parkinson's disease[49], diabetes[50], cardiovascular disease[51], and other diseases associated with oxidative stress, lipid degeneration, and DNA and protein damage. In this study, the incidence and development of ALD in mice triggered by alcohol-induced oxidative stress was successfully inhibited by knocking down *Cyp2e1* in mice using si-*Cyp2e1* LNPs, which has strong implications for other diseases caused by oxidative stress.

Based on our study, it has been shown that ALD can present with liver injury and liver fat accumulation within 4 weeks of alcohol exposure (Table S1 and Fig. S2). After 8 weeks of alcohol feeding, the liver damage and steatosis were further aggravated in mice, mice developed severe alcoholic fatty liver. And the degree of alcoholic liver injury and fatty liver in mice further deepened as the time of alcohol exposure was further extended to 12 weeks (Table S1 and

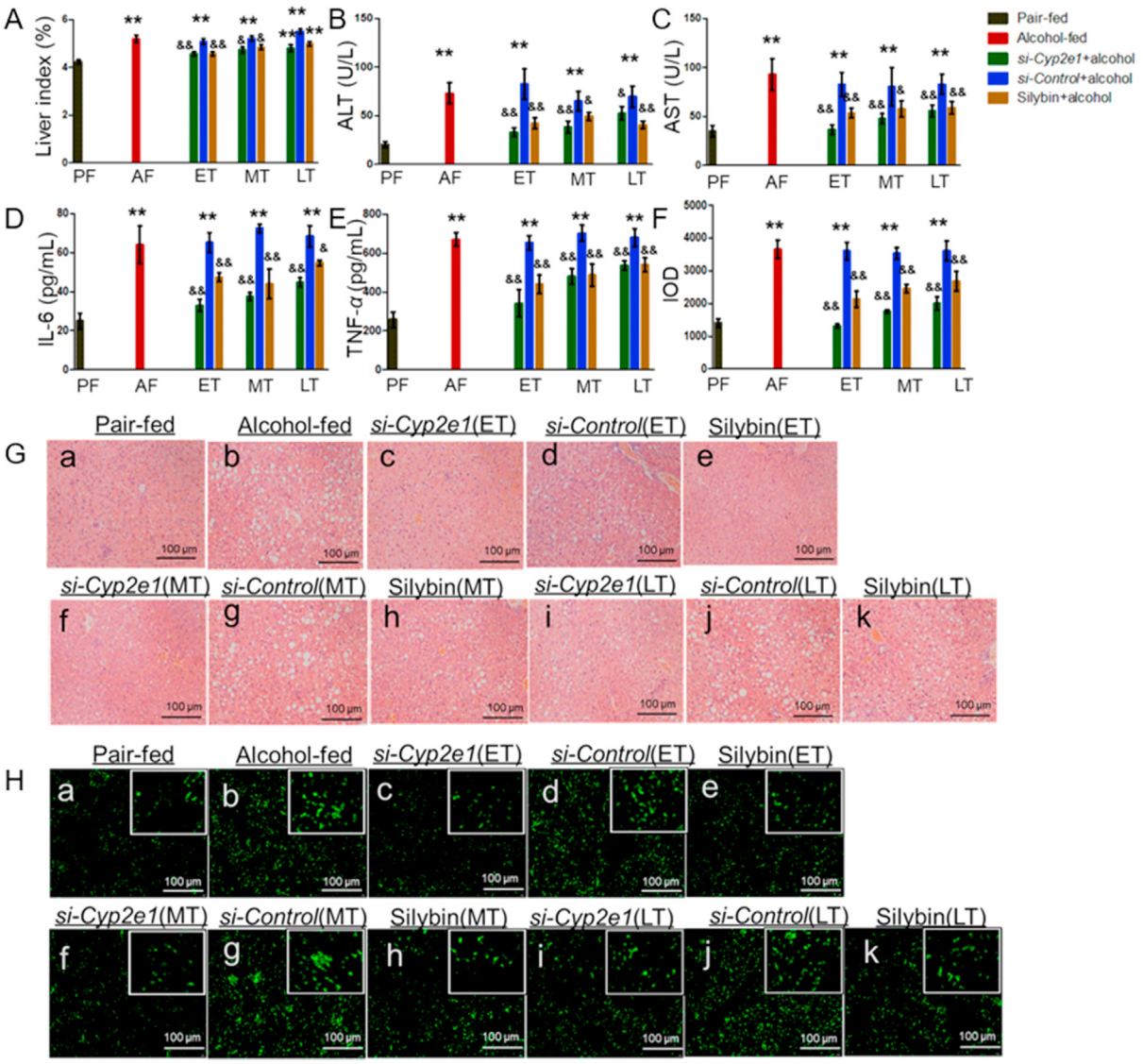

Figure 4 si-*Cyp2e1* LNPs alleviate chronic alcohol-induced liver injury. (A) The levels of liver index ($n = 6$ per group). (B) and (C) The levels of serum AST and ALT ($n = 6$). (D) and (E) The levels of serum IL-6 and TNF-α ($n = 6$). (F) The area of the cumulative optical density (IOD) value in the liver were quantified ($n = 6$). (G) Liver histology analysis with H&E staining. (H) Liver histology analysis with F4/80 fluorescent immunohistochemical staining. Sections were photographed at 200× magnification (scale bars = 100 μm). Each value is the group mean ± SD ($n = 6$). One-way ANOVA with Student's *t*-test. $^{**}P < 0.01$ *versus* pair-fed; and $^{\&}P < 0.05$ and $^{\&\&}P < 0.01$ *versus* alcohol-fed.

Fig. S2). In summary, different degrees of alcoholic liver injury and fatty liver can be induced in mice depending on the exact time period of exposure. In the present study, mice were fed the Lieber-DeCarli ethanol liquid diet and given alcoholic gavage twice a week. After 12 weeks of alcohol feeding, an ALD mouse model was successfully constructed. This model had liver injury and fatty liver with mild inflammatory response and fibrotic response. The mice were divided into three different stages of administration: early-treatment group, mid-treatment group, and late-treatment group. The three stages were injected with si-*Cyp2e1* LNPs through the tail vein. Our results show that si-*Cyp2e1* LNPs had a significant therapeutic effect on the mouse ALD, where the early-treatment group showed the best treatment outcome. si-*Cyp2e1* LNPs intervention in the later stage of ALD also has a good therapeutic effect. Thus, the earlier the drug was administered, the more pronounced the protective effect was.

It has been reported that alcohol-induced hepatocellular injury is mainly caused by ROS and local inflammation, leading to structural and functional damage to the liver and ultimately to increased hepatocellular damage[21,52,53]. Excessive ROS target polyunsaturated fatty acids on the cell membrane, thus producing MDA, as the main product of lipid peroxidation induced by ROS, MDA is used as a biomarker of oxidative stress[54]. The higher the level of MDA, the more serious the lipid peroxidation of the cell membrane is. SOD, GSH, and GSH-Px are reducing agents, that directly neutralize the toxic active products and are involved in maintaining the redox balance of the cells[55]. In this study, the levels of ROS, MDA, SOD, GSH, and GSH-Px in the liver tissues of experimental animals in each group were examined. It was shown that alcohol could lead to a significant increase in MDA and a significant decrease in SOD, GSH-Px, and GSH levels. This indicates that the antioxidant capacity of the liver was reduced

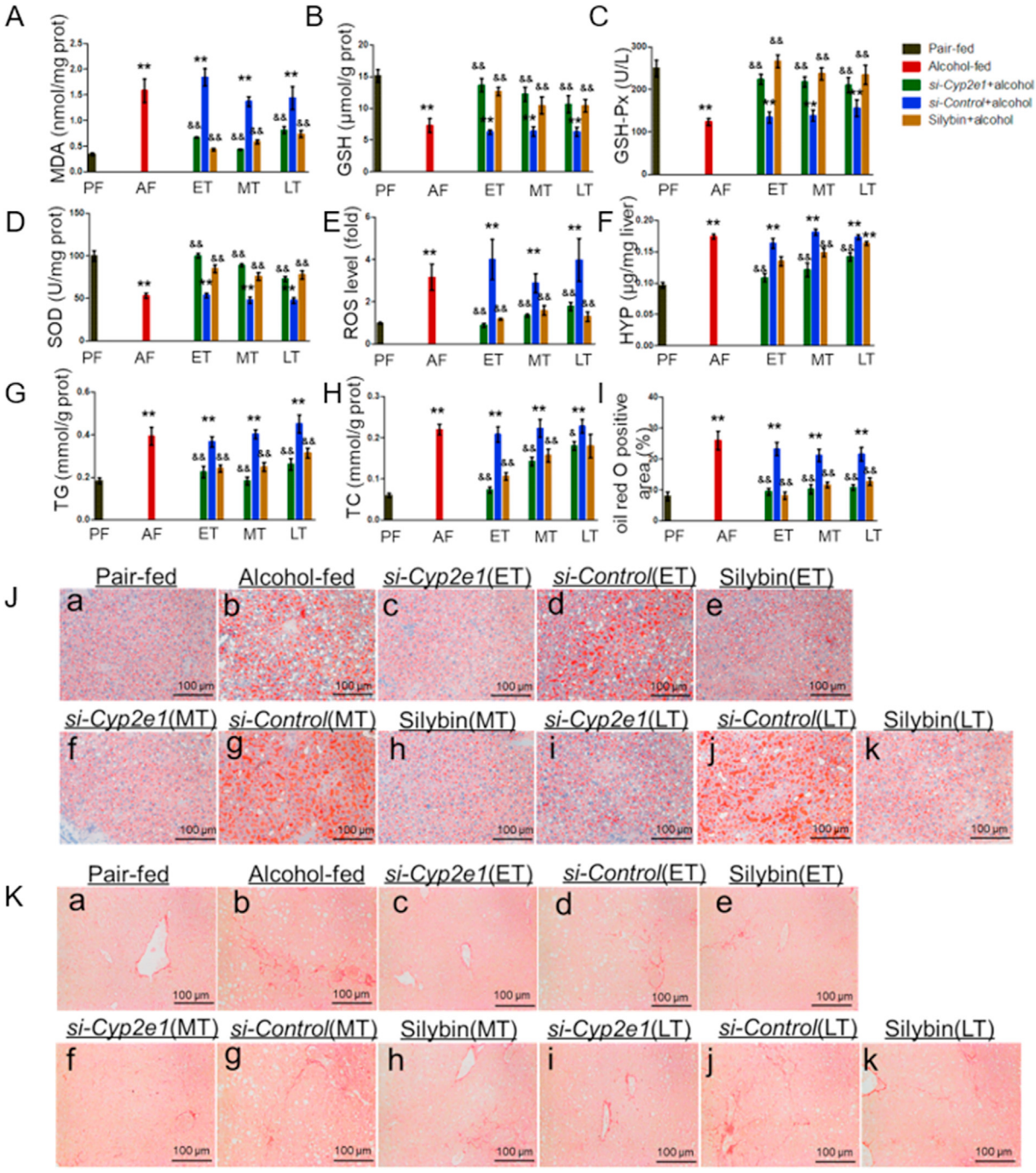

Figure 5 Effect of si-*Cyp2e1* LNPs on liver lipid levels with alcoholic liver injury. (A−E) The levels of liver MDA, GSH, GSH-Px, SOD, and ROS ($n = 6$). (F) The levels of liver hydroxyproline (HYP) ($n = 6$). (G) and (H) The levels of liver TG and TC ($n = 6$). (I) The area of adipocyte infiltration in the same visual field and the situation of fat hoarding in the liver were quantified ($n = 6$). (J) Liver histology analysis with oil red O staining. (E) Liver histology analysis with H&E staining. (K) Liver histology analysis with Sirius red staining (arrows point to fibrosis). Sections were photographed at 200× magnification (scale bar = 100 μm). Each value is the group mean ± SD ($n = 6$). One-way ANOVA with Student's *t*-test. $^{**}P < 0.01$ *versus* pair-fed; and $^{\&}P < 0.05$ and $^{\&\&}P < 0.01$ *versus* alcohol-fed.

and that lipid peroxidation had occurred. Meanwhile, the administration of si-*Cyp2e1* LNPs in different stages of ALD could effectively alleviate this damage to some extent. In particular, the early-treatment group showed significantly upregulated levels of SOD, GSH-Px, and GSH with alcoholic liver injury, and a reduced level of MDA, indicating the significant restoration of the antioxidant capacity of the liver. The important enzymes for the synthesis of ROS are NADPH oxidases, which are composed of membrane-related subunits such as P47phox, P67phox, and GP91phox[56]. The system of scavenging excess free radicals in the organism is composed of antioxidant enzymes such as Gshpx, Gshrd, and Sod1[57]. Our results showed that alcohol can

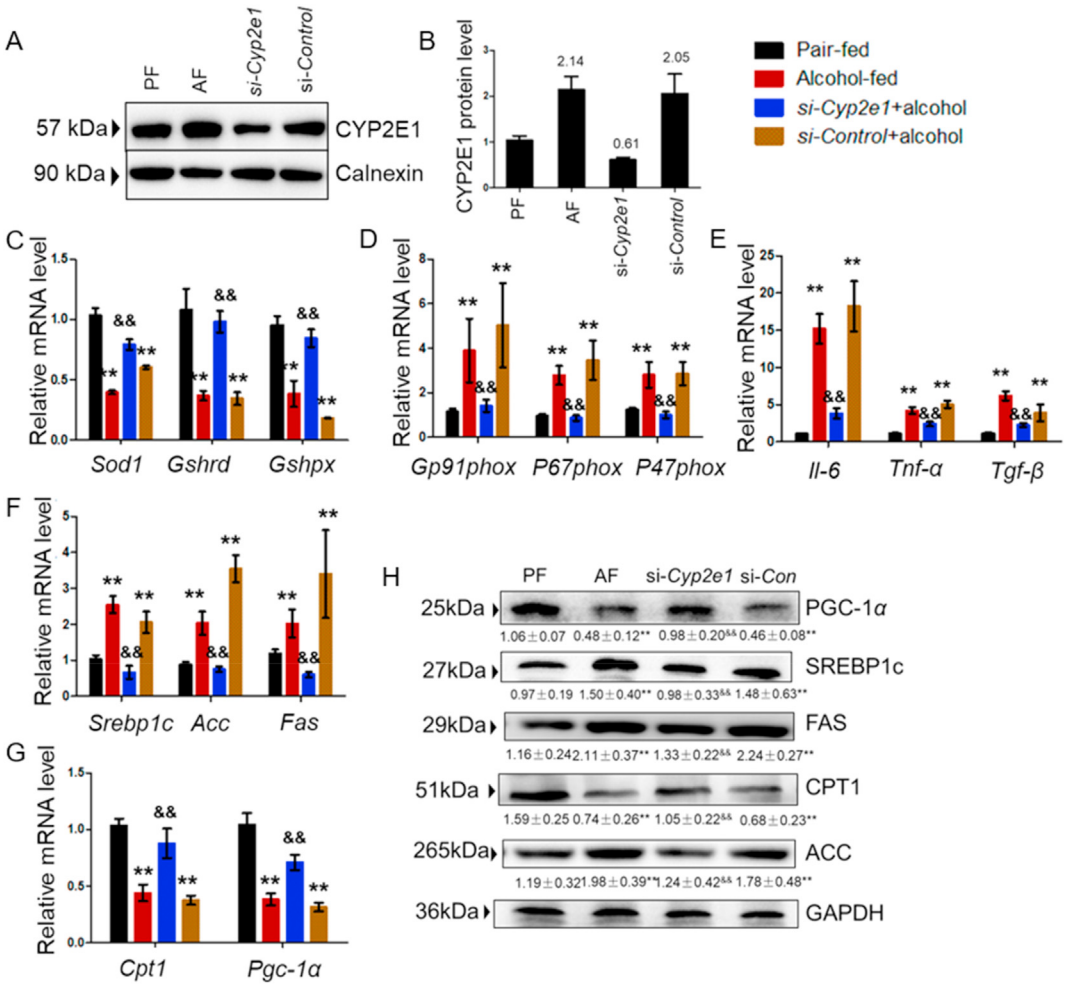

Figure 6 Effect of si-*Cyp2e1* LNPs on the expression of genes related to oxidative stress and steatosis. Mouse liver microsomes, total RNA and total protein were prepared from the livers of mice in the pair-fed group, alcohol-fed group, si-*Cyp2e1* LNPs (early-treatment) group, and si-*Control* LNPs (early-treatment) group. (A) and (B) The protein expression levels of Cyp2e1. (C) The mRNA expression levels of *Gshpx*, *Gshrd* and *Sod1* genes ($n = 6$). (D) The mRNA expression of *P47phox*, *P67phox* and *Gp91phox* genes ($n = 6$). (E) The mRNA expression levels of *Il-6*, *Tnf-α* and *Tgf-β* genes ($n = 6$). (F) The mRNA expression levels of *Srebp1c*, *Acc* and *Fas* genes ($n = 6$). (G) The mRNA expression levels of *Cpt1* and *Pgc-1α* genes ($n = 6$). (H) The protein expression levels of SREBP1c, FAS, ACC, PGC-1α and CPT1 ($n = 6$). Each value is the group mean ± SD ($n = 6$). One-way ANOVA with Student's *t*-test. $^{**}P < 0.01$ *versus* pair-fed; and $^{\&\&}P < 0.01$ *versus* alcohol-fed.

significantly increase oxidative stress, and si-*Cyp2e1* LNPs inhibited the increase of alcohol-induced mRNA expression of *P47phox*, *P67phox*, and *Gp91phox* genes, and restored the expression levels of *Gshpx*, *Gshrd*, and *Sod1* genes to their normal levels. Thus, the levels of ROS and the associated oxidative stress were reduced by si-*Cyp2e1* LNPs.

Long-term alcohol intake may also lead to liver lipid metabolism disorders. An abnormal elevation of TG and TC in the liver was found. The liver index reflects the degree of liver injury under certain conditions[58]. Pathological sections showed that the liver tissue of pair-fed mice was normal, while the livers of alcohol-fed mice showed obvious pathological changes, such as a large number of lipid droplet vacuoles, inflammatory cell infiltration, large-area lipid-droplet accumulation, and slight liver fibrosis, which is consistent with the previous studies[59,60]. The si-*Cyp2e1* LNPs significantly improved these lesions in different stages of ALD.

Some studies have found that the expression of SREBP1c, a known key transcription factor regulating lipid synthesis in the liver, was upregulated in acute alcohol-induced fatty liver, which led to lipid accumulation[61,62]. In the liver tissue of patients with fatty liver, the expression of SREBP1c is five times higher than that of the normal control group[63]. The downstream targets of SREBP1c are ACC and FAS, both essential enzymes for fatty acid synthesis[64,65]. It was suggested that alcohol consumption can increase the expression of SREBP1c in mouse liver, thereby upregulating the gene expression of ACC and FAS, and increasing the synthesis of FA and TG[66,67]. PGC-1α mainly regulates energy metabolism *in vivo* and is a key regulator of mitochondrial production[68]. At the same time, the activation of PGC-1α can also promote the expression of downstream genes related to fatty acid oxidation. CPT1 is a rate-limiting enzyme of fatty acid β-oxidation, which can make long-chain acetyl CoA enter mitochondria, promote fatty acid β-oxidation, produce ATP, and maintain the energy balance between cell and body[69]. The results suggest that alcohol can gradually affect the expression of genes related to lipid synthesis and decomposition in the liver. si-*Cyp2e1* LNPs inhibit liver-fat synthesis-related

genes and increase the expression of fatty-acid metabolism-related genes, reduce liver fat production and accelerate fat metabolism, eventually blocking the development of the alcohol-induced fatty liver.

In this study, introducing si-*Cyp2e1* LNPs at different times of ALD while maintaining continuous alcohol intake showed a better overall ALD treatment effect, where the effect becames more profound with earlier administration. Compared with silymarin, si-*Cyp2e1* LNPs showed better treatment outcomes in the middle and late stages of ALD, coupled with better therapeutic effects on pathological features such as liver inflammation and fibrosis. Additionally, the once-a-week treatment frequency of si-*Cyp2e1* LNPs greatly reduces the frequency of dosing compared to other treatments for ALD. This, in turn, has the potential to improve the patient's medication compliance and increase the feasibility of drug treatment for ALD. Targeting *Cyp2e1* by siRNA LNPs attenuated chronic alcohol-induced steatosis, inflammation, and liver fibrosis, validating that effective *Cyp2e1* mRNA inhibition *in vivo* could enable treatment of ALD and that *Cyp2e1* mRNA as a key target has an important guideline for the development of ALD therapeutics in the future. This is the first report evaluating the efficacy of siRNA LNPs in attenuating alcohol-associated liver disease. Although the regulation of CYP2E1 by many traditional and natural drugs has been extensively studied in cellular and animal models, none of them have been clinically applied. The si-*Cyp2e1* LNP achieved a more efficient and durable regulatory effect of *Cyp2e1* mRNA *in vivo* and alleviated ALD, illustrating the great potential of RNAi therapy in developing new therapeutics in the future. However, only *in vivo* efficacy studies have been performed on si-*Cyp2e1* LNPs. Thus, additional trials for *in vivo* safety assessment are being considered at a later stage.

5. Conclusions

In conclusion, RNAi-based targeting of *Cyp2e1* expression can effectively inhibit the development of ALD in mouse models, validating the feasibility of RNAi as a potential therapeutic tool.

Acknowledgments

This work is kindly supported by The National Key R&D Program of China: Chinese-Australian 'Belt and Road' Joint Laboratory on Traditional Chinese Medicine for the Prevention and Treatment of Severe Infectious Diseases (2020YFE0205100, China), Key project at central government level: The ability establishment of sustainable use for valuable Chinese medicine resources (2060302, China), Zhenjiang social development project (SH2020036, China), National Key R&D Program of China (2019YFA0802801 and 2018YFA0801401, China), the National Natural Science Foundation of China (31871345 and 32071442, China), Medical Science Advancement Program (Basic Medical Sciences) of Wuhan University (TFJC2018004, China), the Fundamental Research Funds for the Central Universities (China), the Non-profit Central Research Institute Fund of Chinese Academy of Medical Sciences (2020-PT320-004, China), Applied Basic Frontier Program of Wuhan City (2020020601012216, China), Hubei Health Commission Young Investigator award (China) and startup funding from Wuhan University (China). We appreciate the helpful discussion and great technical support from Professor Song Shen from School of Pharmacy of Jiangsu University (Zhenjiang, China).

Author contributions

Yalan Wang designed the research, carried out the experiments, performed data analysis, and wrote the manuscript. Qiubing Chen, Shuang Wu, and Xinyu Sun participated part of the experiments. Runting Yin and Zhen Ouyang contributed to formal analysis. Yin Hao and Yuan Wei designed and supervised the experiments and performed data analysis. Yalan Wang, Qiubing Chen, Runting Yin, Yin Hao, and Yuan Wei revised the manuscript. All authors have read and approved the final manuscript.

Conflicts of interest

The authors declare no conflicts of interest.

Appendix A. Supporting information

Supporting data to this article can be found online at https://doi.org/10.1016/j.apsb.2023.01.009.

References

1. Crabb DW, Im GY, Szabo G, Mellinger JL, Lucey MR. Diagnosis and treatment of alcohol-associated liver diseases: 2019 practice guidance from the American association for the study of liver diseases. *Hepatology* 2020;**71**:306−33.
2. Thursz M, Kamath PS, Mathurin P, Szabo G, Shah VH. Alcohol-related liver disease: areas of consensus, unmet needs and opportunities for further study. *J Hepatol* 2019;**70**:521−30.
3. Seitz HK, Bataller R, Cortez-Pinto H, Gao B, Gual A, Lackner C, et al. Alcoholic liver disease. *Nat Rev Dis Primers* 2018;**4**:16.
4. Jinjuvadia R, Liangpunsakul S. Trends in alcoholic hepatitis-related hospitalizations,financial burden, and mortality in the United States. *J Clin Gastroenterol* 2015;**49**:506−11.
5. Warren KR, Murray MM. Alcoholic liver disease and pancreatitis: global health problems being addressed by the US National Institute on Alcohol Abuse and Alcoholism. *J Gastroenterol Hepatol* 2013;**28**(Suppl 1):4−6.
6. Stickel F, Moreno C, Hampe J, Morgan MY. The genetics of alcohol dependence and alcohol-related liver disease. *J Hepatol* 2017;**66**:195−211.
7. Naveau S, Chollet-Martin S, Dharancy S, Mathurin P, Jouet P, Piquet MA, et al. A double-blind randomized controlled trial of infliximab associated with prednisolone in acute alcoholic hepatitis. *Hepatology* 2004;**39**:1390−7.
8. Vonghia L, Leggio L, Ferrulli A, Bertini M, Gasbarrini G, Addolorato G, et al. Acute alcohol intoxication. *Eur J Intern Med* 2008;**19**:561−7.
9. Tighe SP, Akhtar D, Iqbal U, Ahmed A. Chronic liver disease and silymarin: a biochemical and clinical review. *J Clin Transl Hepatol* 2020;**8**:454−8.
10. Yan J, Nie Y, Luo M, Chen Z, He B. Natural compounds: a potential treatment for alcoholic liver disease?. *Front Pharmacol* 2021;**12**:694475.
11. Singal AK, Bataller R, Ahn J, Kamath PS, Shah VH. ACG clinical guideline: alcoholic liver disease. *Am J Gastroenterol* 2018;**113**:175−94.
12. Morgan ET, Devine M, Skett P. Changes in the rat hepatic mixed function oxidase system associated with chronic ethanol vapor inhalation. *Biochem Pharmacol* 1981;**30**:595−600.

13. Koop DR, Morgan ET, Tarr GE, Coon MJ. Purification and characterization of a unique isozyme of cytochrome P-450 from liver microsomes of ethanol-treated rabbits. *J Biol Chem* 1982;**257**:8472−80.
14. Khani SC, Zaphiropoulos PG, Fujita VS, Porter TD, Koop DR, Coon MJ. cDNA and derived amino acid sequence of ethanol-inducible rabbit liver cytochrome P-450 isozyme 3a (P-450ALC). *Proc Natl Acad Sci U S A* 1987;**84**:638−42.
15. Nebert DW, Nelson DR, Coon MJ, Estabrook RW, Feyereisen R, Fujii-Kuriyama Y, et al. The P450 superfamily: update on new sequences, gene mapping, and recommended nomenclature. *DNA Cell Biol* 1991;**10**:1−14.
16. Faut M, Rodriguez de Castro C, Bietto FM, Castro JA, Castro GD. Metabolism of ethanol to acetaldehyde and increased susceptibility to oxidative stress could play a role in the ovarian tissue cell injury promoted by alcohol drinking. *Toxicol Ind Health* 2009;**25**:525−38.
17. Hidestrand M, Shankar K, Ronis MJ, Badger TM. Effects of light and dark beer on hepatic cytochrome P-450 expression in male rats receiving alcoholic beverages as part of total enteral nutrition. *Alcohol Clin Exp Res* 2005;**29**:888−95.
18. Seitz HK, Wang XD. The role of cytochrome P450 2E1 in ethanol-mediated carcinogenesis. *Subcell Biochem* 2013;**67**:131−43.
19. Mitchell T, Chacko B, Ballinger SW, Bailey SM, Zhang J, Darley-Usmar V. Convergent mechanisms for dysregulation of mitochondrial quality control in metabolic disease: implications for mitochondrial therapeutics. *Biochem Soc Trans* 2013;**41**:127−33.
20. Lu Y, Cederbaum AI. CYP2E1 and oxidative liver injury by alcohol. *Free Radic Biol Med* 2008;**44**:723−38.
21. Morgan K, French SW, Morgan TR. Production of a cytochrome P450 2E1 transgenic mouse and initial evaluation of alcoholic liver damage. *Hepatology* 2002;**36**:122−34.
22. Lu Y, Wu D, Wang X, Ward SC, Cederbaum AI. Chronic alcohol-induced liver injury and oxidant stress are decreased in cytochrome P4502E1 knockout mice and restored in humanized cytochrome P4502E1 knock-in mice. *Free Radic Biol Med* 2010;**49**:1406−16.
23. Lu Y, Zhuge J, Wang X, Bai J, Cederbaum AI. Cytochrome P450 2E1 contributes to ethanol-induced fatty liver in mice. *Hepatology* 2008;**47**:1483−94.
24. Ye Q, Wang X, Wang Q, Xia M, Zhu Y, Lian F, et al. Cytochrome P4502E1 inhibitor, chlormethiazole, decreases lipopolysaccharide-induced inflammation in rat Kupffer cells with ethanol treatment. *Hepatol Res* 2013;**43**:1115−23.
25. Gouillon Z, Lucas D, Li J, Hagbjork AL, French BA, Fu P, et al. Inhibition of ethanol-induced liver disease in the intragastric feeding rat model by chlormethiazole. *Proc Soc Exp Biol Med* 2000;**224**:302−8.
26. Stresser DM, Perloff ES, Mason AK, Blanchard AP, Dehal SS, Creegan TP, et al. Selective time- and NADPH-dependent inhibition of human CYP2E1 by clomethiazole. *Drug Metab Dispos* 2016;**44**:1424−30.
27. Greil W, Zhang X, Stassen H, Grohmann R, Bridler R, Hasler G, et al. Cutaneous adverse drug reactions to psychotropic drugs and their risk factors—a case-control study. *Eur Neuropsychopharmacol* 2019;**29**:111−21.
28. Heinemann F, Assion HJ. Hepatotoxic side-effect of clomethiazole. *Pharmacopsychiatry* 1996;**29**:196−7.
29. Seitz H, Mueller S, Nicolas H, Schroeder F, Moreira B, Teng H, et al. Inhibition of cytochrome P-4502E1 by clomethiazole improves alcoholic liver disease in alcohol-dependent patients: a short-term, randomized, controlled clinical trial. *J Hepatol* 2020;**73**:S178−9.
30. Chen X, Mangala LS, Rodriguez-Aguayo C, Kong X, Lopez-Berestein G, Sood AK. RNA interference-based therapy and its delivery systems. *Cancer Metastasis Rev* 2018;**37**:107−24.
31. Akhtar S, Benter IF. Nonviral delivery of synthetic siRNAs *in vivo*. *J Clin Invest* 2007;**117**:3623−32.
32. Xie P, Sun L, Oates PJ, Srivastava SK, Kanwar YS. Pathobiology of renal-specific oxidoreductase/myo-inositol oxygenase in diabetic nephropathy: its implications in tubulointerstitial fibrosis. *Am J Physiol Renal Physiol* 2010;**298**:1393−404.
33. Bucciarelli LG, Kaneko M, Ananthakrishnan R, Harja E, Lee LK, Hwang YC, et al. Receptor for advanced-glycation end products: key modulator of myocardial ischemic injury. *Circulation* 2006;**113**:1226−34.
34. Zoulikha M, Xiao Q, Boafo GF, Sallam MA, Chen Z, He W. Pulmonary delivery of siRNA against acute lung injury/acute respiratory distress syndrome. *Acta Pharm Sin B* 2022;**12**:600−20.
35. Charbe NB, Amnerkar ND, Ramesh B, Tambuwala MM, Bakshi HA, Aljabali AAA, et al. Small interfering RNA for cancer treatment: overcoming hurdles in delivery. *Acta Pharm Sin B* 2020;**10**:2075−109.
36. Takabatake Y, Isaka Y, Mizui M, Kawachi H, Takahara S, Imai E. Chemically modified siRNA prolonged RNA interference in renal disease. *Biochem Biophys Res Commun* 2007;**363**:432−7.
37. Zeigerer A, Gilleron J, Bogorad RL, Marsico G, Nonaka H, Seifert S, et al. Rab5 is necessary for the biogenesis of the endolysosomal system *in vivo*. *Nature* 2012;**485**:465−70.
38. Liu Y, Zhou Q, Zhong L, Lin H, Hu MM, Zhou Y, et al. ZDHHC11 modulates innate immune response to DNA virus by mediating MITA-IRF3 association. *Cell Mol Immunol* 2018;**15**:907−16.
39. Bogorad RL, Yin H, Zeigerer A, Nonaka H, Ruda VM, Zerial M, et al. Nanoparticle-formulated siRNA targeting integrins inhibits hepatocellular carcinoma progression in mice. *Nat Commun* 2014;**5**:3869.
40. Bertola A, Mathews S, Ki SH, Wang H, Gao B. Mouse model of chronic and binge ethanol feeding (the NIAAA model). *Nat Protoc* 2013;**8**:627−37.
41. Lazaro R, Wu R, Lee S, Zhu NL, Chen CL, French SW, et al. Osteopontin deficiency does not prevent but promotes alcoholic neutrophilic hepatitis in mice. *Hepatology* 2015;**61**:129−40.
42. Thompson KJ, Nazari SS, Jacobs WC, Grahame NJ, McKillop IH. Use of a crossed high alcohol preferring (cHAP) mouse model with the NIAAA-model of chronic-binge ethanol intake to study liver injury. *Alcohol Alcohol* 2017;**52**:629−37.
43. Tipoe GL, Liong EC, Casey CA, Donohue Jr TM, Eagon PK, So H, et al. A voluntary oral ethanol-feeding rat model associated with necroinflammatory liver injury. *Alcohol Clin Exp Res* 2008;**32**:669−82.
44. Livak KJ, Schmittgen TD. Analysis of relative gene expression data using real-time quantitative PCR and the 2(-Delta Delta C(T)) Method. *Methods* 2001;**25**:402−8.
45. Ding XX, Coon MJ. Immunochemical characterization of multiple forms of cytochrome P-450 in rabbit nasal microsomes and evidence for tissue-specific expression of P-450s NMa and NMb. *Mol Pharmacol* 1990;**37**:489−96.
46. Gu J, Weng Y, Zhang QY, Cui H, Behr M, Wu L, et al. Liver-specific deletion of the NADPH-cytochrome P450 reductase gene: impact on plasma cholesterol homeostasis and the function and regulation of microsomal cytochrome P450 and heme oxygenase. *J Biol Chem* 2003;**278**:25895−901.
47. Akinc A, Querbes W, De S, Qin J, Frank-Kamenetsky M, Jayaprakash KN, et al. Targeted delivery of RNAi therapeutics with endogenous and exogenous ligand-based mechanisms. *Mol Ther* 2010;**18**:1357−64.
48. Wieckowska A, McCullough AJ, Feldstein AE. Noninvasive diagnosis and monitoring of nonalcoholic steatohepatitis: present and future. *Hepatology* 2007;**46**:582−9.
49. Navarro-Mabarak C, Camacho-Carranza R, Espinosa-Aguirre JJ. Cytochrome P450 in the central nervous system as a therapeutic target in neurodegenerative diseases. *Drug Metab Rev* 2018;**50**:95−108.
50. Zong H, Armoni M, Harel C, Karnieli E, Pessin JE. CytochromeP-450 CYP2E1 knockout mice are protected against high-fat diet-induced obesity and insulin resistance. *Am J Physiol Endocrinol Metab* 2012;**302**:E532−9.
51. Ren J, Pei Z, Chen X, Berg MJ, Matrougui K, Zhang QH, et al. Inhibition of CYP2E1 attenuates myocardial dysfunction in a murine model of insulin resistance through NLRP3-mediated

regulation of mitophagy. *Biochim Biophys Acta, Mol Basis Dis* 2019; **1865**:206−17.
52. Lieber CS. Alcoholic fatty liver: its pathogenesis and mechanism of progression to inflammation and fibrosis. *Alcohol* 2004;**34**:9−19.
53. Wang L, Khambu B, Zhang H, Yin XM. Autophagy in alcoholic liver disease, self-eating triggered by drinking. *Clin Res Hepatol Gastroenterol* 2015;**39 (Suppl 1)**:S2−6.
54. Tsikas D. Assessment of lipid peroxidation by measuring malondialdehyde (MDA) and relatives in biological samples: analytical and biological challenges. *Anal Biochem* 2017;**524**:13−30.
55. Wu G, Fang YZ, Yang S, Lupton JR, Turner ND. Glutathione metabolism and its implications for health. *J Nutr* 2004;**134**:489−92.
56. Louvet A, Mathurin P. Alcoholic liver disease: mechanisms of injury and targeted treatment. *Nat Rev Gastroenterol Hepatol* 2015;**12**: 231−42.
57. Ghezzi P, Bonetto V, Fratelli M. Thiol-disulfide balance: from the concept of oxidative stress to that of redox regulation. *Antioxid Redox Signal* 2005;**7**:964−72.
58. Aruna K, Rukkumani R, Varma PS, Menon VP. Therapeutic role of cuminum cyminum on ethanol and thermally oxidized sunflower oil induced toxicity. *Phytother Res* 2005;**19**:416−21.
59. Ding RB, Tian K, Huang LL, He CW, Jiang Y, Wang YT, et al. Herbal medicines for the prevention of alcoholic liver disease: a review. *J Ethnopharmacol* 2012;**144**:457−65.
60. Derdak Z, Lang CH, Villegas KA, Tong M, Mark NM, de la Monte SM, et al. Activation of p53 enhances apoptosis and insulin resistance in a rat model of alcoholic liver disease. *J Hepatol* 2011;**54**: 164−72.
61. Zeng T, Zhang CL, Song FY, Zhao XL, Yu LH, Zhu ZP, et al. PI3K/Akt pathway activation was involved in acute ethanol-induced fatty liver in mice. *Toxicology* 2012;**296**:56−66.
62. Krycer JR, Sharpe LJ, Luu W, Brown AJ. The Akt-SREBP nexus: cell signaling meets lipid metabolism. *Trends Endocrinol Metab* 2010;**21**: 268−76.
63. DeBose-Boyd RA, Ye J. SREBPs in lipid metabolism, insulin signaling, and beyond. *Trends Biochem Sci* 2018;**43**:358−68.
64. Chirala SS, Hua Chang MM, Abu-Elheiga L, Mao J, Mahon K, Finegold M, et al. Fatty acid synthesis is essential in embryonic development: fatty acid synthase null mutants and most of the heterozygotes die *in utero*. *Proc Natl Acad Sci U S A* 2003;**100**:6358−63.
65. Abu-Elheiga L, Matzuk MM, Kordari P, Oh W, Shaikenov T, Gu Z, et al. Mutant mice lacking acetyl-CoA carboxylase 1 are embryonically lethal. *Proc Natl Acad Sci U S A* 2005;**102**:12011−6.
66. Ji C, Chan C, Kaplowitz N. Predominant role of sterol response element binding proteins (SREBP) lipogenic pathways in hepatic steatosis in the murine intragastric ethanol feeding model. *J Hepatol* 2006;**45**:717−24.
67. Deng QG, She H, Cheng JH, French SW, Koop DR, Xiong S, et al. Steatohepatitis induced by intragastric overfeeding in mice. *Hepatology* 2005;**42**:905−14.
68. Canto C, Auwerx J. AMP-activated protein kinase and its downstream transcriptional pathways. *Cell Mol Life Sci* 2010;**67**:3407−23.
69. Shao H, Mohamed EM, Xu GG, Waters M, Jing K, Ma Y, et al. Carnitine palmitoyltransferase 1A functions to repress FoxO transcription factors to allow cell cycle progression in ovarian cancer. *Oncotarget* 2016;**26**:3832−46.